Synthetic routes to TEG-substituted diketopyrrolopyrrole-based low band gap polymers

Angela Punzi,[a] Francesca Nicoletta,[b] Giuseppe Marzano,[a] Cosimo G. Fortuna,[b] Janardan Dagar,[c] Thomas M. Brown[c] and Gianluca M. Farinola*[a,d]

Abstract: We report general synthetic routes to novel TEG-functionalized DPP-based co-polymers alternating TEG-substituted DPP moieties with various functionalized donor units, such as polythiophene segments decorated with thermocleavable tertiary esters or additional TEG chains and alkoxy-substituted benzodithiophene units. The protocols proposed are based on Stille coupling or, for the first time for TEG-substituted DPP-based polymers, on direct heteroarylation polymerization. Spectroscopic and electrochemical characterization as well as preliminary tests in photovoltaic cells are reported.

Introduction

Low band gap conjugated polymers attract interest as active materials in various organic electronic devices. Usually, they are regular donor-acceptor (D-A) copolymers with alternating electron deficient and electron rich units along the polymer backbone, that exhibit a relatively low band gap associated with an intramolecular charge transfer transition between the electron rich and electron deficient units. Particularly, due to their ability to harvest a large portion of the solar spectrum, several low band-gap polymers have been profitably used as electron-donor components in polymer-based solar cells with high power conversion efficiencies (PCEs).[1] Moreover, D-A conjugated polymers with field-effect mobilities exceeding 1 $cm^2V^{-1}s^{-1}$ have been reported.[2] Although the π-conjugated backbone principally determines the optoelectronic properties of the polymers, recently the role of side chains, primarily utilized as solubilizing groups, for fine tuning of polymers' electronic and spectroscopic properties (e.g. absorption, emission, energy level, molecular packing and charge transport) has been pointed out.[3]

Among electron deficient units, diketopyrrolo[3,4-*c*]pyrrole (DPP) moiety has been widely used as a building block in the synthesis of a variety of D-A type low band-gap polymers.[4] These have been employed in solution processed organic solar cells[5] with PCEs up to 8.0%[5a,e] and in high-performance organic thin film transistors (OTFTs).[6] The DPP moiety is a polar bicyclic electron deficient conjugated unit with a strong propensity to π-stack. It offers many possibility of structural modifications, such as introduction of side chains on the lactam N-atoms for improving solution processability, but also connection with various conjugated blocks at the 2- and 5- positions.[7] N-substituents of the lactam rings of DPP-based derivatives play a critical role in molecular packing which, in turn, affect the charge transport properties of these compounds.[8] Although alkyl chains are the most commonly used solubilizing chains, polar triethylene glycol (TEG) chains have been recently reported as good stack-inducing agents on the DPP units.[9] For example, a DPP-based copolymer functionalized with TEG side chains for high-mobility organic field-effect transistors (electron mobilities of up to 3 $cm^2V^{-1}s^{-1}$) was reported by S. Patil,[9b] while Y. Yang demonstrated that the strong self-assembling effect awarded by TEG side chain is capable to improve the photovoltaic performance in a given polymer system (PCE from 6.2% to 7.0% with TEG modification).[9c] Despite this evidence, only very few examples of TEG-functionalized DPP-based polymers have been reported so far.[8c,9b-d] In the case of molecular DPP derivatives, the introduction of hydrophilic oligoether chains also confers processability in environmental friendly polar solvents and extend the uses of DPP dyes in aqueous solution for biological applications.[10] Recently, we have synthesized new triazole-diketopyrrolopyrrole conjugated molecules functionalized with side chains of various structure and polarity (hydrophobic alkyl chains, hydrophilic triethylene glycol chains and thermocleavable *tert*-butoxycarbonyl (BOC) groups) at both the terminal triazole rings and lactam N atoms, potentially useful for green optoelectronics and biological applications due to their solubility in environmental friendly polar solvents such as alcohols or water.[11] We have also investigated the formation of nanostructured aggregates and dependence of their spectroscopic behavior on the substitution pattern.[11] Here, in

[a] Dipartimento di Chimica, Università degli Studi di Bari Aldo Moro, Via Orabona 4, I-70126 Bari, Italy
E-mail: gianlucamaria.farinola@uniba.it
http://www.chimica.uniba.it
[b] Dipartimento di Scienze Chimiche, Università degli Studi di Catania, Viale A. Doria 6, 95125 Catania, Italy
[c] CHOSE (Centre for Hybrid and Organic Solar Energy), Dipartimento di Ingegneria Elettronica, Università degli studi Roma - Tor Vergata, Via del Politecnico 1, 00133 Roma, Italy.
[d] CNR-ICCOM Istituto di Chimica dei Composti Organometallici, Via Orabona 4, I-70126 Bari, Italy

Supporting information for this article is given via a link at the end of the document.

connection with our previous studies on organometallic methods for the synthesis of conjugated polymers,[12] we report general synthetic protocols to novel DPP-based polymers alternating TEG-substituted DPP moieties with various functionalized donor units, such as polythiophene segments decorated with thermocleavable tertiary esters or additional TEG chains and alkoxy-substituted benzodithiophene units. The spectroscopic and electrochemical characteristics of the synthesized polymers are also investigated and some preliminary tests in photovoltaic devices are described. In fact, although the interest in oligoether side chains was initially attributed to their hydrophilicity and their ability to confer solubility in polar solvents without using ionic groups, it has been shown that oligoether chains greatly affect the self-assembly behavior of the materials and, in turn, their photophysical properties.[8,9,11]

Results and Discussion

We report here a general synthetic protocol to TEG-substituted DPP-based polymers based on the Stille coupling reaction. We also show for the first time the possibility to obtain this class of compounds by a direct heteroarylation polymerization (DHAP).[13] In fact, despite DHAP has already been successfully used to prepare a number of N-alkyl DPP-based copolymers,[14] to the best of our knowledge, this is the first example of use of direct heteroarylation polymerization in preparation of N-TEG DPPs. As shown in Scheme 1, the synthetic route to **TegDPPV**, **TegDPPT** and **TegDPPBDT** is based on a Stille coupling reaction involving 3,6-bis(5-bromothiophen-2-yl)-2,5-bis(2-(2-(2-methoxyethoxy)ethoxy)ethyl)pyrrolo[3,4-*c*]pyrrole-1,4(*2H,5H*)-dione **1**[11] as starting reagent. These polymers were synthesized by coupling the monomer **1** with (*E*)-1,2-bis(tributylstannyl)ethene **2**, 2,5-bis(trimethylstannyl)thiophene **3** and (4,8-bis((2-ethylhexyl)oxy)benzo[1,2-b:4,5-b']dithiophene-2,6-diyl)bis(trimethylstannane) **4**, respectively. All the cross-coupling reactions were performed in anhydrous toluene at 110°C in the presence of 3% amount of $Pd(PPh_3)_4$ as the palladium catalyst leading to the target polymers in moderate to excellent yields (38-90%) after purification by Soxhlet extractions.

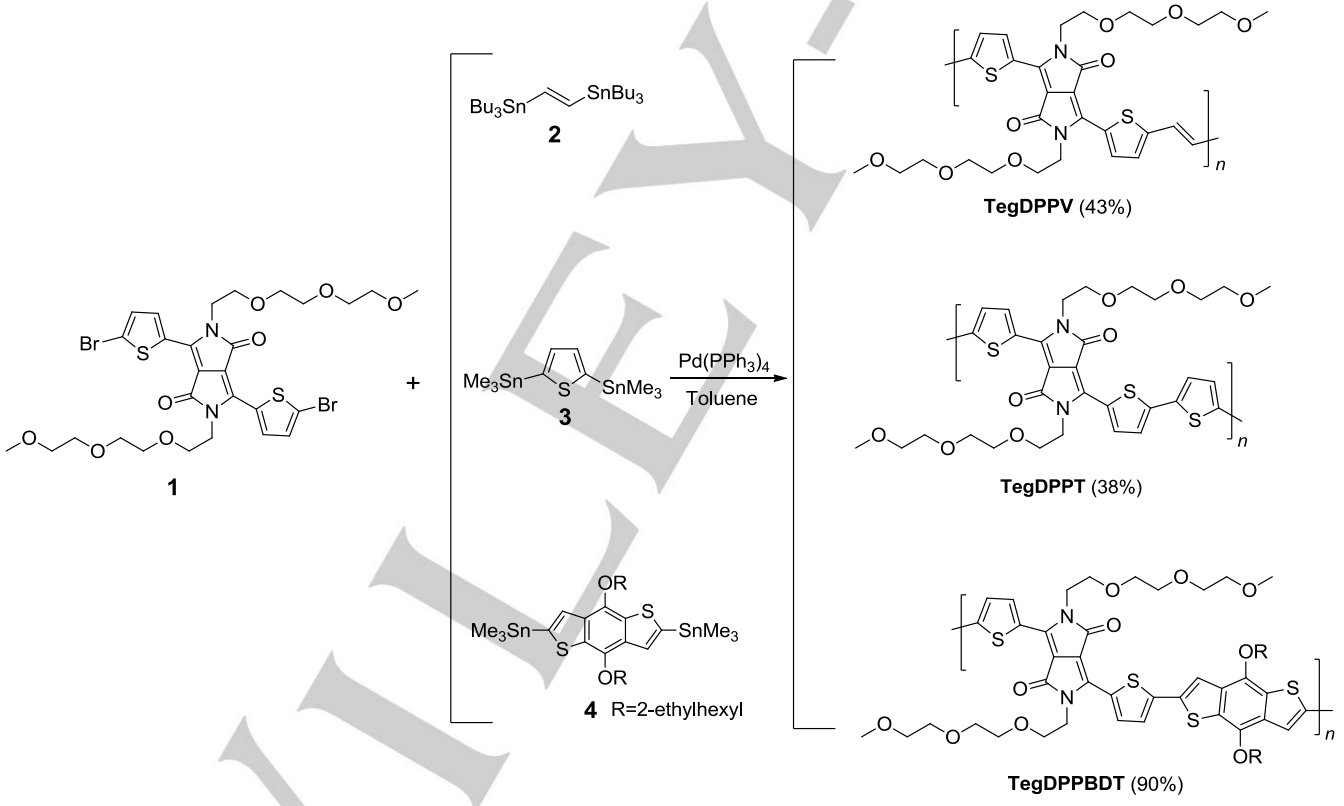

Scheme 1. Synthetic route to **TegDPPV**, **TegDPPT** and **TegDPPBDT**.

The random copolymers **TegDPPTegES** and **TegDPPK**, containing additional polar side chain, were synthesized through Stille coupling reactions of **1** and 2,5-bis(trimethylstannyl)thiophene **3** with 2-(2-(2-methoxyethoxy)ethoxy)ethyl 2,5-dibromothiophene-3-carboxylate **5** or 4-(2,3-bis((*tert*-butyldimethylsilyl)oxy)propoxy)-2-methylbutan-2-yl 2,5-dibromothiophene-3-carboxylate **6**,[15] respectively (Scheme 2).

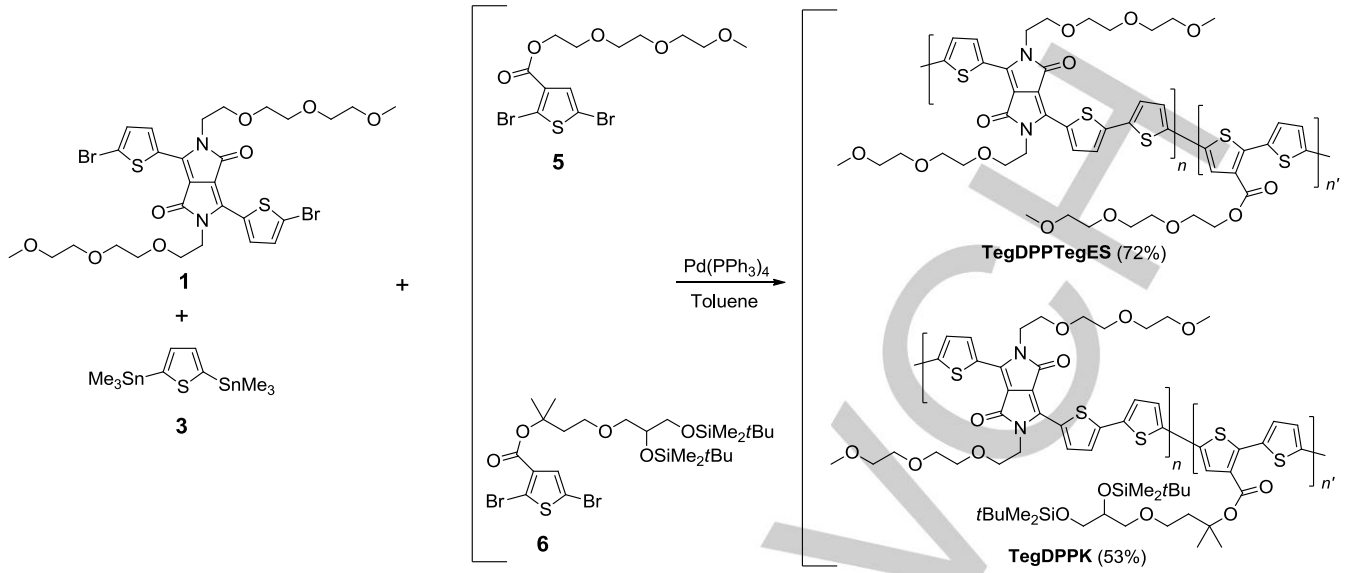

Scheme 2. Synthetic route to **TegDPPTegES** and **TegDPPK**.

We also demonstrated the possibility to synthesize **TegDPPK1** by DHAP. There is a growing interest in direct arylation reactions due to the possibility to overcome most of the issues related to the use of organometallic reagents, especially the high costs associated with the synthesis of the organometallic intermediates. In addition, direct arylation processes result highly attractive for scaling up the synthesis of conjugated polymers to industrial production.[13,14] In agreement with this intriguing synthetic procedure the dibromo derivative **6** was reacted directly with the compound **7**, which does not need to be converted into the corresponding organometallic derivative, leading to polymer **TegDPPK1** (Scheme 3).

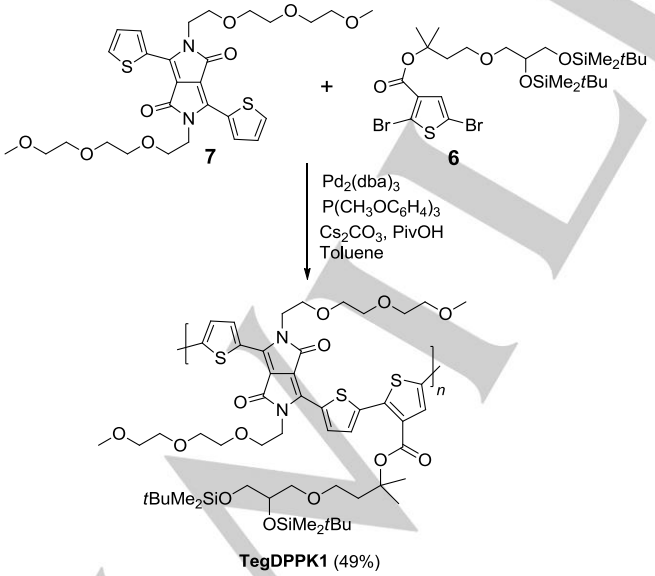

Scheme 3. Synthetic route to **TegDPPK1**.

TegDPPK and **TegDPPK1,** differing in the extension of polythiophene blocks, are decorated with functionalized side chains which, in principle, can be further elaborated by deprotection of the alcoholic functionalities or complete thermal cleavage of the tertiary ester groups.[15] All the synthesized polymers are soluble in halogenated solvents (e.g. chloroform, dichloromethane). Deprotection of the alcoholic groups of **TegDPPK** and **TegDPPK1**, as detailed in the Experimental section, does not significantly increase the solubility in polar solvents.

The molecular weight and polydispersity index of the synthesized polymers were determined by GPC with polystyrene as a standard. Analysis was carried out at room temperature using a mixture of chloroform and DMF (1:0.2 v/v) as eluent in order to minimize the retention of polymers in the GPC column (polymers were not eluted when pure chloroform was used as eluent likely due to their strong interactions with the stationary phase and/or aggregation effects). The GPC analysis (ESI, Figures S1-S6) showed for **TegDPPTegES** and **TegDPPV** the presence of both polymeric and oligomeric species with markedly different molecular weights (bimodal molecular-weight distribution). The polymers **TegDPPT**, **TegDPPBDT**, **TegDPPK** and **TegDPPK1** exhibited similar number average molecular weight (M_n) ranging from 13.0 kDa to 18.5 kDa and polydispersity index (PDI) ranging from 1.6-3.2 (Table 1). Molecular weight of N-TEG DPP polymers obtained by Stille coupling reaction in our experiments are lower compared to the N-alkyl DPP-based polymers described in the literature. This observation suggests that the polyether chains may not confer sufficient solubility to the growing polymer chain in the reaction media, resulting in precipitation of oligomeric and/or low molecular weight polymeric species. In support of this hypothesis, a reduction of the molecular weight of a given polymeric system after a relevant increase of the percentage of TEG chains has been reported by Y. Yang.[9c]

Table 1. GPC data for DPP-based polymers.

Polymer	M_n (kDa)	M_w (kDa)	PDI
TegDPPV[a]	20.3/1.1	29.4/1.3	1.4/1.2
TegDPPT	16.1	25.4	1.6
TegDPPBDT	18.5	42.9	2.3
TegDPPTegES[a]	21.5/1.2	28.4/1.8	1.3/1.5
TegDPPK	13.0	41.3	3.2
TegDPPK1	14.7	31.3	2.1

[a] Bimodal molecular weight distribution was observed.

The spectroscopic properties of the polymers were investigated by UV-Vis-NIR absorption spectroscopy in dilute chloroform solutions and in films spin-coated on quartz slides (1000 rpm/60 s, then 2000 rpm/60 s). The normalized UV-Vis-NIR spectra of TegDPP-based polymers are shown in Figure 1 and the corresponding optical data are summarized in Table 2. It can be seen from Figure 1 that all the absorption spectra in dilute chloroform solution appear as visible to near-infrared absorption with maximum absorption peaks located at wavelengths greater than 700 nm, with the exception of **TegDPPK1** which has a maximum absorption peak at 658 nm. Moreover, Figure 1 shows that all polymers in films exhibit shoulder peaks and extended absorption onsets in the NIR region, which can be attributed to aggregates formed in the solid state. These effects are very pronounced for **TegDPPK1** and also, although to a lesser extent, for **TegDPPV** and **TegDPPBDT**, as it can be seen by comparing the spectra in solution and the corresponding spectra in the solid state. Notably, the analysis of the literature data concerning alkylated analogues of **TegDPPBDT**[16] and **TegDPPV**[17] seems to indicate that the TEG chains are able to produce a greater red shift of absorption onset in the solid state with respect to the alkyl chains. From the onset of the thin film absorptions we estimated the optical bandgaps of polymers in the solid state (Table 2). Low optical bandgaps (E_g^{opt}) ranging from 1.19 and 1.28 were calculated for **TegDPPV**, **TegDPPBDT**, **TegDPPTegES** and **TegDPPK**. **TegDPPK1** shows a larger E_g^{opt} with respect to **TegDPPK** due to a lower extension of polythiophene donor blocks.

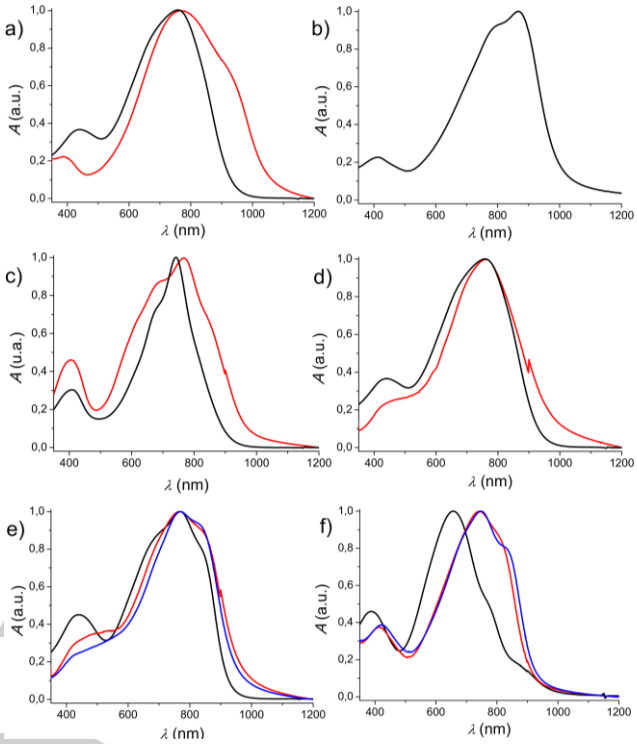

Figure 1: UV-Vis-NIR normalized spectra of **TegDPPV** (a), **TegDPPT** (b), **TegDPPBDT** (c), **TegDPPTegES** (d), **TegDPPK** (e) and **TegDPPK1** (f) in $CHCl_3$ solution (black line) and in the solid state (red line); UV-Vis-NIR normalized spectra of **TegDPPK** (e) and **TegDPPK1** (f) films after thermal treatment at 300 °C for 30 seconds are also reported (blue line).

Table 2. Optical data of TegDPP-based polymers.

Polymer	$\lambda_{max\ sol}$ (nm)[a]	$\lambda_{onset\ sol}$ (nm)[a]	$\lambda_{max\ film}$ (nm)[b]	$\lambda_{onset\ film}$ (nm)[b]	E_g^{opt} (eV)[c]
TegDPPV	756	935	777[d]	1043	1.19
TegDPPT	869	1000	-[e]	-[e]	-[e]
TegDPPBDT	743	900	765[f]	971	1.28
TegDPPTegES	758	941	760[g]	976	1.27
TegDPPK	771	912	777[h]	975	1.27
TegDPPK1	658	880	741[i]	918	1.35

[a] measured in diluite $CHCl_3$ solution; [b] films deposited by spin-coating from $CHCl_3$ solution; [c] optical bandgap evaluated as $E_g = 1240/\lambda_{onset\ film}$; [d] film from $CHCl_3$ solution (10mg/mL); [e] for **TegDPPT** it was not possible to acquire the UV-Vis-NIR spectrum in the solid state due to its poor wettability; [f] film from $CHCl_3$ solution (6mg/mL); [g] film from $CHCl_3$ solution (5mg/mL); [h] film from $CHCl_3$ solution (3.5mg/mL); [i] film from $CHCl_3$ solution (5mg/mL).

The thermal decomposition characteristics of **TegDPPK** and **TegDPPK1**, both bearing thermally cleavable tertiary ester groups, were investigated. **TegDPPK** and **TegDPPK1** films, spin coated from chloroform solution, were heated on a hot plate at 300 °C for 30 seconds in air. After thermal treatment, only slight

differences in the absorption profile were observed, as shown in Figure 1, while a drastic reduction of solubility in chloroform was detected due to the thermal cleavage of the ester side chains as suggested by IR analysis (Figure 2). This result is very interesting since the removal of flexible side chains improve solvent resistance leading to morphologically more stable films. Additionally, removing excess insulating side chains might improve the charge transport properties of polymers.[3] The thermal stability of **TegDPPK** and **TegDPPK1** was also investigated by thermal gravimetric analysis (TGA). The TGA analysis in air for **TegDPPK** reveals the loss of 25% in weight, in the range of 240-400 °C due to the thermolysis of the ester side chain. The same occurs for **TegDPPK1** in the range of 220-290 °C, with the loss of 28% in weight (Figure 3).

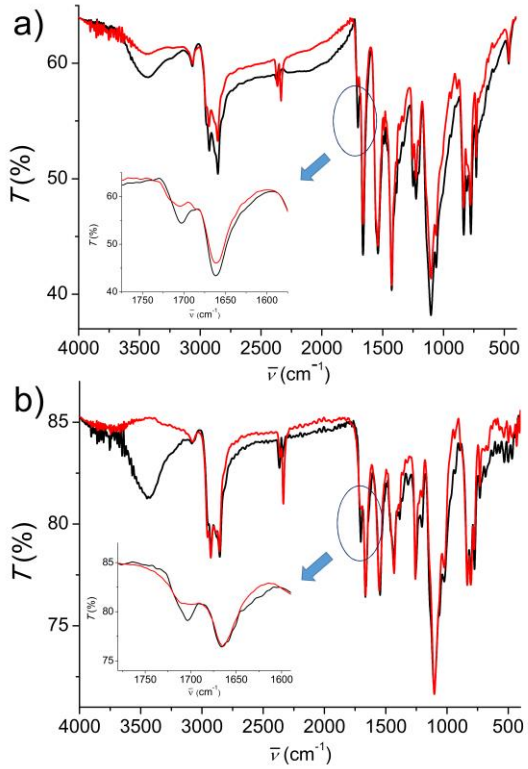

Figure 2. FT-IR spectra of **TegDPPK** (a) and **TegDPPK1** (b) before (black) and after thermal cleavage at 300 °C for 30 seconds (red).

Electrochemical properties and HOMO and LUMO energy levels of polymers were measured by cyclic voltammetry (CV). Figure 4 showed the CV curves of the polymer films on platinum working electrodes in 0.1 M tetrabutylammonium hexafluorophosphate (*n*-Bu_4NPF_6)/acetonitrile solution. All measurements were calibrated using the Fc/Fc^+ redox couple as external standard. The HOMO and LUMO energy levels were estimated using the following empirical equations: $E_{HOMO} = -e(E_{ox} + 5.1V)$ and $E_{LUMO} = -e(E_{red} + 5.1V)$ where E_{ox} is the onset oxidation potential *vs* Fc/Fc^+ and E_{red} is the onset reduction potential *vs* Fc/Fc^+ and -5.1eV is the position of the formal potential of the Fc/Fc^+ redox couple in the Fermi scale.[18] The E_{ox} and E_{red} were determined from the intersection of the two tangents drawn at the rising current and baseline charging current of the CV traces. The results of the electrochemical measurements are summarized in Table 3. The measured electrochemical bandgaps are significantly larger than the corresponding optical bandgaps probably due to the presence of an energy barrier at the interface between the polymer film and the electrode surface.[19] It can be noted that the current intensity for the reduction curves is much lower than that of the oxidation curves. This evidence suggests that the polymers may have a better capability of transporting holes instead of electrons as

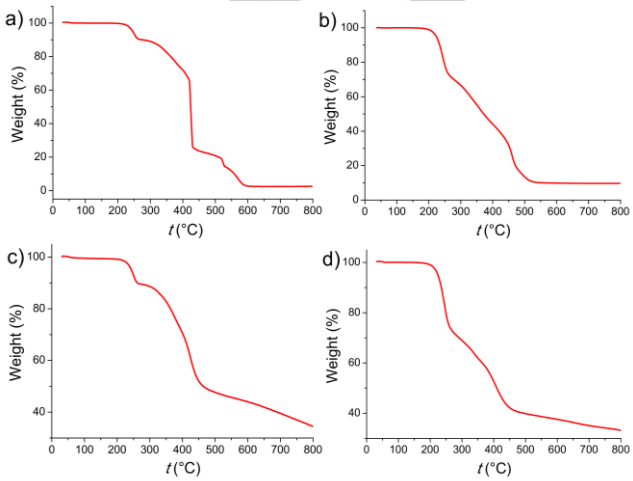

previously also reported for N-alkyl DPP-based polymers.[17]

Figure 3. TGA analysis of **TegDPPK** in air (a) and under nitrogen (c); TGA analysis of **TegDPPK1** in air (b) and under nitrogen (d).

Table 3. Electrochemical data of TegDPP-based polymers.

Polymer	E_{ox} (V)[a]	HOMO (eV)[b]	E_{red} (V)[a]	LUMO (eV)[b]	E_g^{el} (eV)[c]
TegDPPV	0.30	-5.40	-1.25	-3.85	1.55
TegDPPT	0.06	-5.16	-1.31	-3.79	1.37
TegDPPBDT	0.25	-5.35	-1.38	-3.72	1.63
TegDPPTegES	0.12	-5.22	-1.38	-3.72	1.50
TegDPPK	0.25	-5.35	-1.51	-3.59	1.76
TegDPPK1	0.40	-5.50	1.35	-3.75	1.75

[a] Onset oxidation and reduction potentials *vs* Fc/Fc^+; [b] HOMO-LUMO energy levels evaluated as $E_{HOMO} = -e(E^{ox}_{onset} + 5.1V)$ and $E_{LUMO} = -e(E^{red}_{onset} + 5.1V)$ where E_{onset} is measured versus Fc/Fc^+ reference and -5.1eV is the position of the formal potential of the Fc/Fc^+ redox couple in the Fermi scale;[18] [c] Electrochemical band gap calculated from $E_g = -e(E_{ox} - E_{red})$.

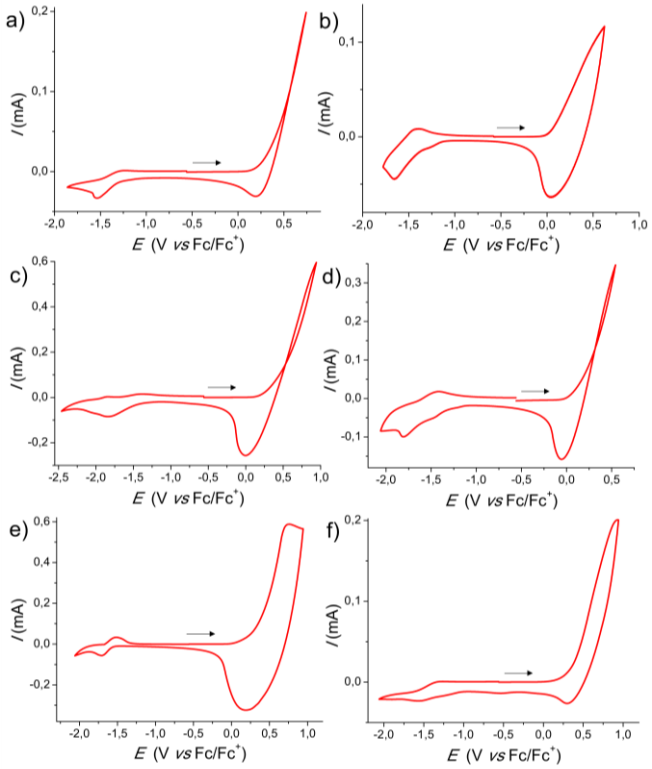

Figure 4: Cyclic voltammograms of **TegDPPV** (a), **TegDPPT** (b), **TegDPPBDT** (c), **TegDPPTegES** (d), **TegDPPK** (e) and **TegDPPK1** (f) films on a Pt working electrode in 0.1M *n*-Bu_4NPF_6/ acetonitrile at room temperature.

Preliminary tests in polymer solar cells with bulk heterojunction configuration (BHJ) have been made using **TegDPPBDT** as the donor material. We decided to use **TegDPPBDT** because of its better characteristics compared to the other polymers. In fact, **TegDPPBDT** is obtained with the highest yield (90%) and the highest degree of polymerization in the absence of multimodal distribution and it shows good solubility in chloroform as well as a good wettability. We have fabricated the following solar cell in the inverted architecture:[20] ITO/ZnO/**TegDPPBDT**:$PC_{70}BM/MoO_3$/Ag. The polymer blend layer was subjected to thermal annealing at 290 °C for 2 minutes in the inert atmosphere. The *J-V* curves in dark and under one sun are shown in Figure 5 for the best performing device. The efficiency and photovoltaic parameters are shown in Table 4 both for the average and the best cell. The best efficiency was 1.56%, which represent an interesting result since it was obtained in not optimized solar cells. A lower annealing temperature (150 °C) provides less satisfactory photovoltaic parameters resulting in lower efficiency (J_{sc} = 2.36 mA/cm^2, V_{oc} = 0.523V, FF = 42.9%, efficiency = 0.53%) as detailed in ESI (Figures S7-S8, Table 1). The analysis of the dark *J-V* curves (ESI, Figure S8-(b)) also shows that the rectification of the solar cell improves at 290 °C with the on/off current ratio increasing from 88 (for the 150 ºC annealed device) to 190.

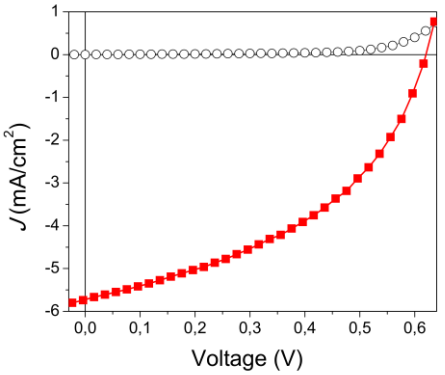

Figure 5: *J-V* characteristics of **TegDPPBDT**:$PC_{70}BM$ based inverted solar cell device in dark (black open circles) and under AM1.5G, 1000 W/m2 illumination (red solid squares).

Table 4. PV parameters for ITO/ZnO/**TegDPPBDT**:$PC_{70}BM/MoO_3$/Ag solar cells under AM1.5G, 1000 W/m^2 illumination.

Device	J_{sc} (mA/cm^2)	V_{oc} (V)	FF (%)	PCE (%)
Average	5.45±0.30	0.598±0.010	41.1±3.1	1.34±0.18
Best	5.71	0.616	44.4	1.56

The external quantum efficiency (EQE) curve shows that the ITO/ZnO/**TegDPPBDT**:$PC_{70}BM/MoO_3$/Ag solar cells have broad spectra spanning the whole visible and near IR with a peak at 520nm (Figure 6). For comparison, the absorption spectrum of the solar cell device has also been recorded (Figure 7).

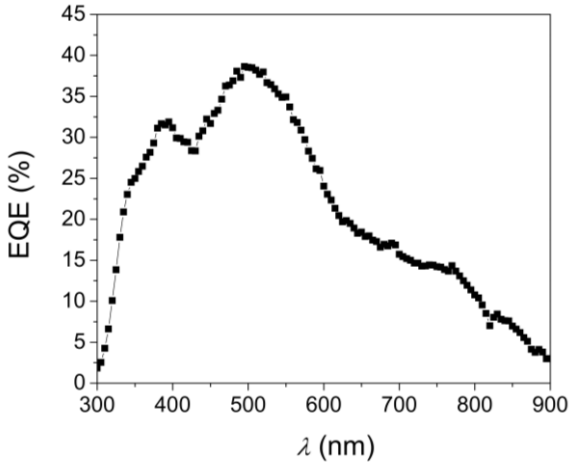

Figure 6: EQE spectrum of ITO/ZnO/**TegDPPBDT**:$PC_{70}BM$ /MoO_3/Ag solar cell.

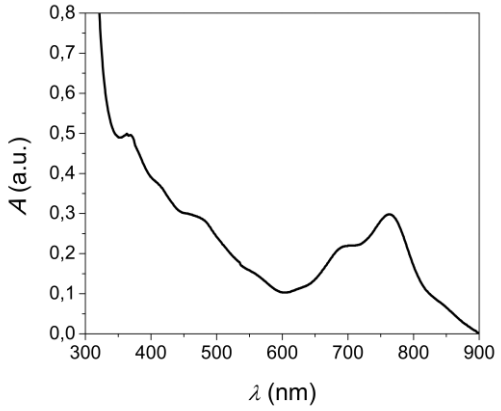

Figure 7: Absorption spectrum of ITO/ZnO/**TegDPPBDT**:$PC_{70}BM$ /MoO_3/Ag solar cell.

Despite **TegDPPBDT** absorbs very well in the NIR region, the photocurrent response is very poor in this part of the spectrum showing that most charge generation comes from the fullerene rather than the polymer. This evidence indicate that there is scope to improve the concentration ratio more towards the donor polymer in order to enhance cell performance. Furthermore, the possibility to improve injection of electrons from the donor to the acceptor molecules with a higher offset between the LUMOs of the two components deserves to be explored. However, we consider a systematic investigation of the devices' parameters to optimize photovoltaic performances out of the scope of this article and it will be reported in due course.

Conclusions

We have developed general synthetic routes to DPP-based copolymers bearing TEG chains on the lactam rings of the DPP units and various functionalized side chains, such as additional TEG chains, thermocleavable tertiary esters or alkoxy groups, on the co-monomers. The polymerization can be performed via Stille coupling. We have also showed that it is possible to successfully use a direct heteroarylation polymerization for the synthesis of this class of DPP-based polymers. DHAP avoids the use of organometallic intermediates and, in turn, it result highly attractive for scaling up the synthesis of conjugated polymers to industrial production. All the polymers synthesized exhibit low band gaps in film with maximum absorption peaks located at wavelengths greater than 700 nm. Shoulder peaks and a more extended absorption in the NIR region are present in absorption spectra of films with respect to the corresponding spectra in solution. These effects are very pronounced for **TegDPPK1**, which exhibit a large red shift of maximum absorption peak, and also, although to a lesser extent, for **TegDPPV** and **TegDPPBDT**. Comparison of our experimental data with literature data concerning alkylated analogues of **TegDPPBDT** and **TegDPPV** seems to indicate that the TEG chains are able to produce a greater red shift of absorption onset in the solid state with respect to the alkyl chains, confirming the importance of the TEG chains as stack-inducing agents. Our experiments on thermal decomposition of **TegDPPK** and **TegDPPK1** showed that it is possible to increase solvent resistance of polymer films by thermal cleavage of the tertiary ester side chains at 300 °C for 30 seconds. Finally, preliminary tests in devices show that **TegDPPBDT** can be profitably used as the donor material in BHJ polymer solar cell.

Experimental Section

General remarks: Reaction solvents were distilled immediately prior to use as follows: chloroform and dichloromethane were dried by distillation from P_2O_5 and toluene was dried by distillation from sodium/benzophenone. Reagents were purchased at the highest commercial quality and used without further purification. 2,5-Dibromothiophene-3-carboxylic acid was prepared according previously reported literature procedure.[21] 4-(2,3-Bis((*tert*-butyldimethylsilyl)oxy)propoxy)-2-methylbutan-2-ol was purchased from Sigma-Aldrich. 2,5-Bis(2-(2-(2-methoxyethoxy)ethoxy)ethyl)-3,6-di(thiophen-2-yl)pyrrolo[3,4-*c*]pyrrole-1,4(*2H,5H*)-dione was purchased from SunaTech Inc. Preparative column chromatography was carried out using Macherey-Nagel silica gel (60, particle size 0.063-0.2 mm). Macherey-Nagel aluminum sheets with silica gel 60 F_{254} were used for TLC analyses. ^{1}H-NMR and ^{13}C-NMR spectra were recorded on a Varian Inova at 400 and at 100.6 MHz, respectively, by using the residual proton peak of $CDCl_3$ at δ = 7.24 ppm as internal standard for ^{1}H spectra and the signals of $CDCl_3$ at δ = 77 ppm as internal standard for ^{13}C spectra of molecular compounds or the residual proton peak of $C_2D_2Cl_4$ at δ = 5.90 ppm as internal standard for ^{1}H spectra of polymers. IR spectra were recorded on a Perkin-Elmer FT-IR Spectrum Bx. High-resolution mass spectra were acquired on a Shimadzu high performance liquid chromatography-ion trap-time of flight mass spectrometer (LCMS-IT-TOF) *via* direct infusion of the samples using methanol as the elution solvent. GPC analysis were carried out on a Malvern Viscotek TDA 305 or on a Knauer Instrument both equipped with a Tosoh Bioscience TSKgel G3000HHR column (7.8mm IDx30.0cm L) using a refractive index or a UV-Vis detector, respectively. TGA analysis were performed in air or under nitrogen on a Perkin-Elmer TGA-7. UV-Vis absorption measurements have been performed on a Shimadzu UV-2401PC spectrophotometer. Solid state UV-vis spectra were acquired depositing polymers onto 1cmx1cm quartz glasses by spin casting (1000 rpm/60 s, then 2000 rpm/60 s) from a chloroform solution. Optical energy band gaps (E_g^{opt}) were estimated from absorption onset wavelengths (E_g = 1240/λ_{onset} (eV)) in films. Cyclic voltammetry measurements were carried out with an Autolab potentiostat (model PGSTAT128N) by Metrohm using a conventional three electrode configuration consisting of a platinum working electrode, a platinum counter electrode and an Ag/AgCl reference electrode. The working electrode was coated with a polymer film by drop-casting a polymer solution in chloroform. The oxidation and reduction cycles were recorded continuously by applying positive potentials and subsequent negative potentials, respectively. All CV measurements were recorded at room temperature under nitrogen atmosphere using a 0.1 M solution of *n*-Bu_4NPF_6 solution in anhydrous acetonitrile as supporting electrolyte (scan rate 0.1 Vs^{-1}). All measurements were calibrated using the Fc/Fc^+ redox couple as external standard. The HOMO and LUMO energy levels were estimated using the following empirical equations: E_{HOMO} = -e(E_{ox} + 5.1V) and E_{LUMO} = -e(E_{red} + 5.1V) where E_{ox} is the onset oxidation potential vs Fc/Fc^+ and E_{red} is the onset reduction potential vs Fc/Fc^+ and -5.1eV is the position of the formal potential of the Fc/Fc^+ redox couple in the Fermi scale.[18]

3,6-Bis(5-bromothiophen-2-yl)-2,5-bis(2-(2-(2-methoxyethoxy)ethoxy)ethyl)pyrrolo[3,4-c]pyrrole-1,4(2H,5H)-dione (1). This compound was synthesized according to modified literature procedures.[9a-c] A round bottom flask covered with aluminium foil and equipped with a magnetic stirrer was charged with a solution of 2,5-bis(2-(2-(2-methoxyethoxy)ethoxy)ethyl)-3,6-di(thiophen-2-yl)pyrrolo[3,4-*c*]pyrrole-1,4(2*H*,5*H*)-dione (1.000g, 1.69mmol) in dry chloroform (30mL). After cooling to 0°C, N-bromosuccinimide (0.602g, 3.38mmol) was added in one portion. The reaction mixture was stirred at 0 °C in the dark for 1h, then quenched with a saturated aqueous solution of NH_4Cl (30 mL), and extracted with dichloromethane (3x60 mL). The organic extracts were washed with an aqueous solution of NaCl (3x30 mL), dried over Na_2SO_4 and concentrated under vacuum. The crude product was purified by washing with several aliquots of methanol. After drying in vacuum, the pure product **1** was obtained as a dark purple solid (0.697g, 55% yield). IR (KBr): ν_{max} 3087, 2898, 2870, 1652, 1555, 1396, 1129, 1119 cm^{-1}; ^1H NMR (400 MHz, $CDCl_3$): δ 8.44 (d, *J* = 4.0Hz, 2H), 7.14 (d, *J* = 4.0 Hz, 2H), 4.11 (t, *J* = 5.8 Hz, 4H), 3.71 (t, *J* = 5.8 Hz, 4H), 3.61-3.56 (m, 4H), 3.55-3.49 (m, 8H), 3.46-3.41 (m, 4H), 3.29 (s, 6H) ; ^{13}C NMR (100.6 MHz, $CDCl_3$): δ 161.1, 139.3, 134.8, 131.2, 131.0, 119.2, 107.8, 71.8, 70.7, 70.5, 70.4, 68.8, 58.9, 42.1 (one coincident peak not observed); LCMS-IT-TOF calculated for $C_{28}H_{34}Br_2N_2O_8S_2$ $(M+Na)^+$: 771.0016, found: m/z 770.9985.

2-(2-(2-Methoxyethoxy)ethoxy)ethyl 2,5-dibromothiophene-3-carboxylate (5). A nitrogen-purged three-necked round bottom flask equipped with a magnetic stirrer was charged with 2,5-dibromothiophene-3-carboxylic acid (0.300g, 1.05mmol), a solution of 2-(2-(2-methoxyethoxy)ethoxy)ethanol (0.132g, 0.81mmol) in dry dichloromethane (6mL) and N,N-dimethylpyridin-4-amine (0.147g, 1.21mmol). The mixture was stirred at room temperature for 1h, then cooled at 0 °C. Dicyclohexylcarbodiimide (0.216g, 1.05mmol) was added under nitrogen and the resulting mixture was stirred at room temperature for 16h. The solvent was removed by evaporation under vacuum, then the crude product was purified by column chromatography on silica gel using a mixture of hexane and ethyl acetate with a volume ratio of 1:1 as eluent. A colorless oil was isolated (0.328g, 93% yield). IR (KBr): ν_{max} 2914, 2873, 1725, 1425, 1223, 1135, 1109, 769 cm^{-1}; ^1H NMR (400 MHz, $CDCl_3$): δ 7.35 (s, 1H), 4.43-4.38 (m, 2H), 3.80-3.76 (m, 2H), 3.70-3.60 (m, 6H), 3.54-3.51 (m, 2H), 3.36 (s, 3H); ^{13}C NMR (100.6 MHz, $CDCl_3$): 160.6, 131.7, 131.5, 119.4, 111.3, 71.9, 70.6, 70.6, 70.5, 68.9, 64.2, 59.0; LCMS-IT-TOF calculated for $C_{12}H_{16}Br_2O_5S$ $(M+Na)^+$: 452.8977, found: m/z 452.8949.

4-(2,3-Bis((tert-butyldimethylsilyl)oxy)propoxy)-2-methylbutan-2-yl 2,5-dibromothiophene-3-carboxylate (6). A nitrogen-purged three-necked round bottom flask equipped with a magnetic stirrer was charged with 2,5-dibromothiophene-3-carboxylic acid (0.150g, 0.52mmol), a solution of 4-(2,3-bis((*tert*-butyldimethylsilyl)oxy)propoxy)-2-methylbutan-2-ol (0.163g, 0.40mmol) in dry dichloromethane (3mL) and N,N-dimethylpyridin-4-amine (0.074g, 0.60mmol). The mixture was stirred at room temperature for 1h, then cooled at 0 °C. Dicyclohexylcarbodiimide (0.108g, 0.52mmol) was added under nitrogen and the resulting mixture was stirred at room temperature for 16h. The solvent was removed by evaporation under vacuum, then the crude product was purified by column chromatography on silica gel using a mixture of hexane and ethyl acetate with a volume ratio of 10:0.5 as eluent. A colorless oil was isolated (0.217g, 80% yield). IR (KBr): ν_{max} 2945, 2928, 2887, 2856, 1711, 1468, 1424, 1386, 1364, 1249, 1136, 1112, 1007, 835, 776 cm^{-1}; ^1H NMR (400 MHz, $CDCl_3$): δ 7.25 (s, 1H), 3.75 (quintet like, *J* = 5.4, 1H), 3.60-3.46 (m, 4H), 3.45-3.40 (m, 1H), 3.36-3.30 (m, 1H), 2.14 (t, *J* = 6.6Hz, 2H), 1.57 (s, 6H), 0.86 (s, 9H), 0.85 (s, 9H), 0.04 (s, 6H), 0.02 (s, 6H); ^{13}C NMR (100.6 MHz, $CDCl_3$): δ 159.8, 133.2, 131.9, 118.1, 111.0, 83.72, 72.9, 72.7, 67.4, 65.0, 40.3, 26.6, 26.5, 25.9, 25.8, 18.3, 18.2, -4.6, -4.7, -5.4, -5.4; LCMS-IT-TOF calculated for $C_{25}H_{46}Br_2O_5SSi_2$ $(M+Na)^+$: 695.0863, found: m/z 695.0856.

General procedure for the synthesis of TegDPPV, TegDPPT, TegDPPBDT. A nitrogen-purged three-necked round bottom flask equipped with a magnetic stirrer and a condenser was charged, under nitrogen, with compound **1** (1 equiv.), distannylated derivative **2**, **3** or **4** (1 equiv.), $Pd(Ph_3)_4$ (0.03 equiv.) and dry toluene. The resulting mixture was warmed at 110°C for 48h. Polymeric chain was end-capped as follow: iodobenzene (5 equiv.) was added and the mixture was stirred at 110 °C for 4h, then 2-tributylstannylthiophene (5 equiv.) was added and the mixture was further stirred at 110 °C for 4h. The reaction mixture was cooled to room temperature and poured in methanol (**TegDPPV** and **TegDPPBDT**) or hexane (**TegDPPT)**, and the solid was recovered by filtration. The crude product was purified by Soxhlet extractions with methanol, acetone, hexane and chloroform in succession. The polymer was obtained as a dark solid from the chloroform fraction by precipitation in methanol (**TegDPPV** and **TegDPPBDT**) or evaporation under vacuum (**TegDPPT)**.

TegDPPV. The polymer was synthesized from compounds **1** (0.600g, 0.80mmol) and **2** (0.486g, 0.80mmol) in dry toluene (15mL) in accordance with the general procedure. Dark blue solid (0.213g, 43% yield). IR (KBr): ν_{max} 2914, 2015, 1657, 1543, 1434, 1402, 1092, 1055 cm^{-1}; ^1H NMR (400 MHz, $C_2D_2Cl_4$, 90°C): δ 8.78-8.67 (m, 2H), 7.29-7.14 (m, 4H), 4.30-4.10 (m, 4H), 3.82-3.70 (m, 4H), 3.68-3.38 (m, 16H), 3.30-3.22 (m, 6H).

TegDPPT. The polymer was synthesized from compounds **1** (0.200g, 0.27mmol) and **3** (0.109g, 0.27mmol) in dry toluene (10mL) in accordance with the general procedure. Dark blue-green solid (69mg, 38% yield). IR (KBr): ν_{max} 2962, 2909, 2845, 1657, 1540, 1530, 1422, 1260, 1095, 1055, 1020, 800 cm^{-1}; ^1H NMR (400 MHz, $C_2D_2Cl_4$, 90°C): δ 8.80-8.60 (m, 2H), 7.35-7.10 (m, 6H), 4.29-4.16 (m, 4H), 3.84-3.71 (m, 4H), 3.70-3.38 (m, 16H), 3.29-3.24 (m, 6H).

TegDPPBDT. The polymer was synthesized from compounds **1** (0.200g, 0.27mmol) and **4** (0.192g, 0.27mmol) in dry toluene (10mL) in accordance with the general procedure. Dark blue-green solid (0.252g, 90% yield). IR (KBr): ν_{max} 2914, 2856, 1657, 1543, 1422, 1353, 1099, 1055, 1033 cm^{-1}; ^1H NMR (400 MHz, $C_2D_2Cl_4$, 90°C): δ 9.25-8.60 (m, 2H), 7.55-6.50 (m, 4H), 4.24-3.00 (m, 34H), 1.70-0.85 (m, 30H).

General procedure for the synthesis of TegDPPTegES and TegDPPK. A nitrogen-purged three-necked round bottom flask equipped with a magnetic stirrer and a condenser was charged, under nitrogen, with compound **1** (1 equiv.), distannylated derivative **3** (2 equiv.), dibromide derivative **5** or **6** (1 equiv.), $Pd(Ph_3)_4$ (0.03 equiv.) and dry toluene. The resulting mixture was warmed at 110°C for 48h. Polymeric chain was end-capped as follow: iodobenzene (5 equiv.) was added and the mixture was stirred at 110 °C for 4h, then 2-tributylstannylthiophene (5 equiv.) was added and the mixture was further stirred at 110°C for 4h. The reaction mixture was cooled to room temperature, poured in methanol and the solid was recovered by filtration. The crude product was purified by Soxhlet extractions with methanol, acetone, hexane and chloroform in succession. The polymer was obtained as a dark solid from the chloroform fraction by precipitation in methanol.

TegDPPTegES. The copolymer was synthesized from compounds **1** (0.180g, 0.24mmol), **3** (0.197g, 0.48mmol) and **5** (0.104g, 0.24mmol) in dry toluene (10mL) in accordance with the general procedure. Dark blue-green solid (0.178g, 72% yield). IR (KBr): ν_{max} 2914, 2856, 1700, 1655, 1535, 1422, 1222, 1196, 1095, 1055, 1020 cm^{-1}; ^1H NMR (400 MHz, $C_2D_2Cl_4$, 90°C): δ 8.84-8.63 (m, 2H), 7.64-6.75 (m, 7H), 4.48-4.13 (m, 6H), 3.88-3.20 (m, 39H).

TegDPPK. The copolymer was synthesized from compounds **1** (0.200g, 0.27mmol), **3** (0.218g, 0.53mmol) and **6** (0.179g, 0.27mmol) in dry toluene

(10mL) in accordance with the general procedure. Dark blue-green solid (0.183g, 53% yield). IR (KBr): ν_{max} 2924, 2854, 1702, 1663, 1540, 1427, 1251, 1227, 1107, 1061, 835, 777 cm^{-1}; ^1H NMR (400 MHz, $C_2D_2Cl_4$, 90°C): δ 8.80-8.64 (m, 2H), 7.50-7.04 (m, 10H), 4.30-4.20 (m 4H), 3.84-3.24 (m, 40H), 2.20-2.10 (m, 4H), 1.54 (br s, 12H), 0.84 (br s, 36H), 0.02 (br s, 12H), -0.01 (br s, 12H).

Synthesis of TegDPPK1. A three-necked round bottom flask equipped with a magnetic stirrer and a condenser, was charged with compound **7** (0.200g, 0.34mmol), compound **6** (0.228g, 0.34mmol), Cs_2CO_3 (0.220g, 0.68mmol), tris(4-methoxyphenyl)phosphine (12mg, 0.034mmol) and pivalic acid (11mg, 0.10mmol). The flask was evacuated and backfilled with nitrogen (3 times), then $Pd_2(dba)_3$ (16mg, 0.02mmol) and dry toluene (8mL) were added under nitrogen and the mixture was stirred at 110 °C for 48h. The reaction mixture was cooled to room temperature, poured in methanol and the solid was recovered by filtration. The crude product was purified by Soxhlet extractions with methanol, acetone, hexane in succession. The polymer was obtained as a dark solid from the hexane fraction by precipitation in methanol. Dark blue solid (0.185g, 49% yield). IR (KBr): ν_{max} 2925, 2855, 1792, 1666, 1544, 1434, 1257, 1206, 1103, 1023, 832, 805, 774 cm^{-1}; ^1H NMR (400 MHz, $C_2D_2Cl_4$, 90°C): δ 8.80-8.65 (m, 2H), 7.64-7.54 (m, 2H), 7.38-7.30 (m, 1H), 4.32-4.18 (m, 4H), 3.84-3.70 (m, 4H), 3.68-3.20 (m, 29H), 2.20-2.10 (m, 2H), 1.56 (br s, 6H), 0.84 (br s, 18H), 0.03 (br s, 6H), 0.00 (br s, 6H).

General procedure for the deprotection of the alcoholic groups of TegDPPK and TegDPPK1. A round bottom flask equipped with a magnetic stirrer and a condenser was charged with **TegDPPK** or **TegDPPK1** (1 equiv.), *n*-Bu_4NF (4 equiv.) and THF. The mixture was stirred at 35 °C for 12h. Methanol was added and the mixture was stirred at room temperature for further 24h. Ethyl acetate was dropped to obtain the complete precipitation of deprotected polymer, which was then recovered by filtration. FT-IR analysis was used to monitor the alcoholic groups deprotection.

Deprotected TegDPPK. IR (KBr): ν_{max} 3432, 2914, 2851, 1692, 1647, 1530, 1418, 1381, 1214, 1196, 1092, 1055, 790 cm^{-1}.

Deprotected TegDPPK1. IR (KBr): ν_{max} 3394, 2914, 2869, 1700, 1662, 1540, 1430, 1108, 1060, 731 cm^{-1}.

Organic Solar Cells

Materials: **TegDPPBDT** polymer. $PC_{70}BM$ (99.99%) was purchased from Solenne BV. Zinc oxide nanoparticle dispersion, Molybdenum oxide (MoO_3, 99.98% powder), ortho-dichlorobenzene and silver (Ag, wire Z 99.99%) were purchased from Sigma Aldrich.

Device Fabrication: Inverted solar cell devices were fabricated on ITO coated glass substrate (Kintec -8 Ω/□) patterned with wet-etching in hydrobromic acid (HBr) and cleaned in ultrasonic bath using acetone and isopropanol for 10min one after one. At first, ZnO nanoparticles were deposited on ITO substrate by spin coating at 2500rpm for 45 second and then annealed in air at 140 °C temperature for 40 minutes. Next, the active layer (1:2) of **TegDPPBDT** and $PC_{70}BM$ dissolved in ortho-dichlorobenzene solvent with 3% DIO (1,8-diiodooctane) additive was spin coated at 1000rpm for 60 second and annealed at 290 °C for 2 minutes in the inert atmosphere. At last all devices were transferred inside the metal evaporator where 5nm thick MoO_3 layer and silver contact with 100nm thickness were deposited through the shadow mask in below 10^{-6} mbar pressure. Thus we obtained total 4 devices with 0.1 cm^2 area of each cell.

Measurements: Current density-voltage (*J-V*) characteristics of all solar cell devices were measured by Keithley 2420 under an AM1.5 Class A ABET solar simulator with an intensity of 1000 W/m^2. The EQE measurements were performed using an IPCE (Incident Photon-to-current Conversion Efficiency) system (IPCE-LS200, Dyers) calibrated with a UV-enhanced Si detector (Thorlabs, 250-1100nm).

Acknowledgements

This work was financially supported by Ministero dell'Istruzione, dell'Università e della Ricerca (MIUR) and by Università degli Studi di Bari "Aldo Moro": "PRIN 2012 prot. 2012A4Z2RY (AQUA-SOL)", "PON02_00563_3316357 (PON MAAT)" and "PON03PE_00004_1 (PON MAIND)". The authors thank dr. Massimo Maccagno for the preparation of 2,5-dibromothiophene-3-carboxylic acid and dr. Pasquale Ferrara for preliminary work on synthesis of TegDPP-based polymers by Stille coupling.

Keywords: diketopyrrolopyrroles • low bandgap • polymers • cross-coupling • oligoether chains

[1] a) C. Liu, K. Wang, X. Gong, A. J. Heeger, *Chem. Soc. Rev.* **2016**, DOI: 10.1039/C5CS00650C; b) I. Etxebarria, J. Ajuria, R. Pacios, *Org. Electron.* **2015**, *19*, 34-60; c) E. Zhou, K. Hashimoto, K. Tajima, *Polymer* **2013**, *54* 6501-6509; d) P.-L. T. Boudreault, A. Najari, M. Leclerc, *Chem. Mater*. 2011, *23*, 456-469; e) R. Kroon, M. Lenes, J.C. Hummelen, P. W. M. Blom, B. De Boer, *Polym. Rev.* **2008**, *48*, 531-582; (f) E. Bundgaard, F. C. Krebs, *Sol. Energ. Mat. Sol. C.* **2007**, *91*, 954–985.

[2] a) H, Sirringhaus, *Adv. Mater.* **2014**, *26*, 1319-1335; b) J. Mei, Y. Diao, A.L. Appleton, L. Fang, Z. Bao, *J. Am. Chem. Soc.* **2013**, *135*, 6724-46.

[3] J. Mei, Z. Bao, *Chem. Mater.* **2014**, *26*, 604-615.

[4] a) Y. Li, P. Sonar, L. Murphy, W. Hong, *Energy Environ. Sci.* **2013**, *6*, 1684-1710; b) D. Chandran, K.-S. Lee, *Macromol. Res.* **2013**, *21*, 272-283; c) A. M. Naik, S. Patil, *J. Polym. Sci., Part A: Polym. Chem.* **2013**, *51*, 4241-4260; d) S. Qua, H. Tian, *Chem. Commun.* **2012**, *48*, 3039-3051.

[5] a) J.-H. Kim, M. Lee, H. Yang, D.-H. Hwang, *J. Mater. Chem. A* **2014**, *2*, 6348-6352; b) H. Bronstein, E. Collado-Fregoso, A. Hadipour, Y. W. Soon, Z. Huang, S. D. Dimitrov, R. S. Ashraf, B. P. Rand, S. E. Watkins, P. S. Tuladhar, I. Meager, J. R. Durrant, I. McCulloch, *Adv. Funct. Mater.* **2013**, *23*, 5647-5654; c) J. Li, K.-H. Ong, P. Sonar, S.-L. Lim, G.-M. Ng, H.-K. Wong, H.-S. Tan, Z.-K. Chen, *Polym. Chem.* **2013**, *4*, 804-811; d) J. Ajuria, S. Chavhan, R. Tena-Zaera, J. Chen, A.J. Rondinone, P. Sonar, A. Dodabalapur, R. Pacios, *Org. Electron.* **2013**, 14, 326-334; e) K. H. Hendriks, G. H. L. Heintges, V. S. Gevaerts, M. M. Wienk, R. A. J. Janssen, *Angew. Chem., Int. Ed.* **2013**, *52*, 8341-8344; f) W. W. Li, K. H. Hendriks, W. S. C. Roelofs, Y. Kim, M. M. Wienk, R. a. J. Janssen, *Adv.Mater.* **2013**, *25*, 3182-3186; g) J. W. Jung, F. Liu, T. P. Russell, W. H. Jo, *Energy Environ. Sci*. **2012**, *5*, 6857-6861; h) F. Liu, Y. Gu, C. Wang, W. Zhao, D. Chen, A. L. Briseno, T. P. Russell, *Adv. Mater.* **2012**, *24*, 3947-3951; i) W. W. Li, W. S. C. Roelofs, M. A. Wienk, R.A. J. Janssen, *J. Am. Chem. Soc.* **2012**, *134*, 13787-13795; l) L. Dou, J. Gao, E. Richard, J. You, C.-C. Chen, K. C. Cha, Y. He, G. Li, Y. Yang, *J. Am. Chem. Soc.* **2012**, *134*, 10071-10079; m) L. Dou, J. You, J. Yang, C.-C. Chen, Y. He, S. Murase, T. Moriarty, K. Emery, G. Li, Y. Yang, *Nat. Photon* **2012**, *6*, 180-185; n) X. Zhang, L. J. Richter, D. M. DeLongchamp, R. J. Kline, M. R. Hammond, I. McCulloch, M. Heeney, R. S. Ashraf, J. N. Smith, T. D. Anthopoulos, B. Schroeder, Y. H. Geerts, D. A. Fischer, M. F. Toney, *J. Am. Chem. Soc*. **2011**, *133*, 15073-15084.

[6] C. B. Nielsen, M. Turbiez, I. McCulloch, *Adv. Mater.* **2013**, *25*, 1859-1880.

[7] M. Grzybowski, D. T. Gryko, *Adv. Optical Mater.* **2015**, *3*, 280-320.

[8] a) M. A. Naik, N. Venkatramaiah, C. Kanimozhi, S. Patil, *J. Phys. Chem. C* **2012**, *116*, 26128-26137; b) J. H. Seo, *Synthetic Met.* **2012**, *162*, 748-752; c) C. Kanimozhi, N. Yaacobi-Gross, E. K. Burnett, A. L. Briseno, T. D. Anthopoulos, U. Salznerd, S. Patil, *Phys. Chem. Chem. Phys.* **2014**, *16*, 17253-17265; d) B. Fu, J. Baltazar, A. R. Sankar, P.-H. Chu, S. Zhang, D. M. Collard, E. Reichmanis, *Adv. Funct. Mater.* **2014**, *24*, 3734-3744.

[9] a) J. Me , K. R. Graham, R. Stalde , S. P. Tiwari, H. Cheun, J. Shim, M. Yoshi, C. Nuckolls, B. Kippelen, R. K. Castellano, J. R. Reynolds, *Chem. Mater*. **2011**, *23*, 2285-2288; b) C. Kanimozhi, N. Yaacobi-Gross, K. W. Chou, A. Amassian, T. D. Anthopoulos, S. Patil, *J. Am. Chem. Soc.* **2012**, *134*, 16532-16535; c) W-H. Chang, J. Gao, L. Dou, C-C. Chen, Y. Liu, Y. Yang, *Adv. Energy Mater.* **2014**, *4*, 1300864; d) J. Dhar, C. Kanimozhi, N. Yaccobi-Gross, T. D. Anthopoulos, U. Salzner, S Patil, *Isr. J. Chem.* **2014**, 54, 817-827.

[10] a) J. Schmitt, V. Heitz, A. Sour, F. Bolze, H. Ftouni, J.-F. Nicoud, L. Flamigni, B. Ventura, *Angew. Chem*. **2015**, *127*, 171-175; *Angew. Chem. Int. Ed.* **2015**, *54*, 169-173; b) G. Zhang, L. Song, S. Bi, Y. Wu, J. Yu, L. Wang, *Dyes Pigm.* **2014**, *102*, 100-106; c) G. Zhang, H. Li, S. Bi, L. Song, Y. Lu, L. Zhang, J. Yu, L. Wang, *Analyst*, **2013**, *138*, 6163-6170; d) G. Zhang, S. Bi, L. Song, F. Wang, J. Yu, L. Wang, *Dyes Pigm.,* **2013**, *99*, 779-786; e) H. Ftouni, F. Bolze, J.-F. Nicoud, *Dyes Pigm.* **2013**, *97*, 77-83; f) H. Ftouni, F. Bolze, H. de Rocquigny, J.-F. Nicoud, *Bioconjugate Chem.* **2013**, *24*, 942-950; g) A. Nowak-Krol, M. Grzybowski, J. Romiszewski, M. Drobizhev, G. Wicks, M. Chotkowski, A. Rebane, E. Gorecka, D. T. Gryko, *Chem. Commun.* **2013**, *49*, 8368-8370.

[11] A. Punzi, E. Maiorano, F. Nicoletta, D. Blasi, A. Ardizzone, N. Ventosa, I. Ratera, J. Veciana, G. M. Farinola, *Eur. J. Org. Chem.* **2016**, DOI: 10.1002/ejoc.201600120.

[12] a) C. Martinelli, U. Giovanella, A. Cardone, S. Destri, G. M. Farinola, *Polymer* **2014**, *55*, 5125-5131; b) A. Cardone, C. Martinelli, V. Pinto, F. Babudri, M. Losurdo, G. Bruno, P. Cosma, F. Naso, G.M. Farinola, *J. Polym. Sci., Part A: Polym. Chem.* **2010**, *48*, 285-291; c) G.M. Farinola, F. Babudri, A. Cardone, O. Hassan Omar, F. Naso, *Pure Appl. Chem.* **2008**, *80*, 1735-1746; d) F. Babudri, A. Cardone, G. M. Farinola, C. Martinelli, R. Mendichi, F. Naso, M. Striccoli, *Eur. J. Org. Chem.,* **2008**, *11*, 1977-1982; e) F. Babudri, D. Colangiuli, L. Di Bari, G. M. Farinola, O. Hassan Omar, F. Naso, G. Pescitelli, *Macromolecules* **2006**, *39*, 5206-5212; f) F. Babudri, G. M. Farinola, F. Naso, *J. Mat. Chem.* **2004**, *14,* 11-34.

[13] a) P.-O. Morin, T. Bura, M. Leclerc, *Mater. Horiz.* **2016**, *3*, 11-20; b) F. Grenier, B. R. Aïch, Y.-Y. Lai, M. Guérette, A. B. Holmes, Y. Tao, W. W. H. Wong, M. Leclerc, *Chem. Mater.* **2015**, *27*, 2137-2143; c) G. Marzano, D. Kotowski, F. Babudri, R. Musio, A. Pellegrino, S. Luzzati, R. Po, G. M. Farinola, *Macromolecules* **2015**, *48*, 7039-7048; d) P.-O. Morin, T. Bura, B. Sun, S. I. Gorelsky, Y. Li, M. Leclerc, *ACS Macro Lett.* **2015**, *4*, 21-24; e) G. Marzano, C. V. Ciasca, F. Babudri, G. Bianchi, A. Pellegrino, R. Po, G. M. Farinola, *Eur. J. Org. Chem.* **2014**, *30*, 6583-6614; f) L. G. Mercier, M. Leclerc, *Acc. Chem. Res.* **2013**, *46*, 1597-1605.

[14] a) J. Kuwabara, N. Takase, T. Yasuda, T. Kanbara, *J Polym Sci A Polym Chem* **2016**, DOI: 10.1002/pola.28105; b) Y. Gao, X. Zhang, H. Tian, J. Zhang, D. Yan, Y. Geng, F. Wang, *Adv. Mate*r. **2015**, *27*, 6753-6759; c) S. Broll, F. Nübling, A. Luzio, D. Lentzas, H. Komber, M. Caironi, M. Sommer, *Macromolecules* **2015**, *48*, 7481-7488; d) P. Homyak, Y. Liu, F. Liu, T. P. Russel, E. B. Coughlin, *Macromolecules* **2015**, *48*, 6978-6986; e) K. Wang, G. Wang, M. Wang, *Macromol. Rapid Commun*. **2015**, *36*, 2162-2170; f) M. Gruber, S.-H. Jung, S. Schott, D. Venkateshvaran, A. J. Kronemeijer, J. W. Andreasen, C. R. McNeill, W. W. H. Wong, M. Shahid, M. Heeney, J.-K. Lee, H. Sirringhaus, *Chem. Sci*. **2015**, *6*, 6949-6960; g) J. R. Pouliot, B. Sun, M. Leduc, A. Najari, Y. Li, M. Leclerc, *Polym. Chem.* **2015**, *6,* 278-282; h) P. Sonar, T. Ru, B. Foonga, A. Dodabalapur, *Phys. Chem. Chem. Phys.* **2014**, *16*, 4275-4283; i) J. Kuwabara, Y. Nohara, S. J. Choi, Y. Fujinami, W. Lu, K. Yoshimura, J. Oguma, K. Suenobu, T. Kanbara, *Polym. Chem*. **2013**, *4*, 947-953; l) Q. Guo, J. Dong, D. Wan, D. Wu, J. You, *Macromol. Rapid Commun*. **2013**, *34*, 522-527; m) J. R. Pouliot, L. G. Mercier, S. Caron, M. Leclerc, *Macromol. Chem. Phys*. **2013**, *214*, 453-457.

[15] R. Søndergaard, M. Helgesen, M. Jørgensen, F. C. Krebs, *Adv. Energy Mater.* **2011**, *1*, 68-71.

[16] a) S. Zhang, L. Ye, Q. Wang, Z. Li, X. Guo, L. Huo, H. Fan, J. Hou, *J. Phys. Chem. C* **2013**, *117*, 9550-9557; b) Y. Wang, F. Yang, Y. Liu, R. Peng, S. Chen, Z. Ge, *Macromolecules* **2013**, *46*, 1368-1375; c) J. W. Jung, J. W. Jo, F. Liu, T. P. Russel, W.H. Jo, *Chem. Commun.* **2012**, *48*, 6933-6935.

[17] P.-T. Wu, F. S. Kim, S. A. Jenekhe, *Chem. Mater.* **2011**, *23*, 4618-4624.

[18] C. M. Cardona, W. Li, A. E. Kaifer, D. Stockdale, G. C. Bazan, *Adv. Mater.* **2011**, *23*, 2367-2371.

[19] J. C. Bijleveld, B. P. Karsten, S. G. J. Mathijssen, M. M. Wienk, D. M. de Leeuw, R. A. J. Janssen, *J. Mater. Chem.* **2011**, *21*, 1600-1606.

[20] G. Susanna, L. Salamandra, C. Ciceroni, F. Mura, T. M. Brown, A. Reale , M. Rossi, A. DiCarlo, F. Brunetti, *Sol. Energ. Mat. Sol. C.* **2015**, *134*, 194-198.

[21] D.-S. Kim, K. H. Ahn, *J. Org. Chem.* **2008**, *73*, 6831-6834.

Entry for the Table of Contents

FULL PAPER

General synthetic routes to DPP-based copolymers bearing TEG chains on the DPP units and variously functionalized side chains (e.g. TEG chains, thermocleavable tertiary esters or alkoxy groups) on the co-monomers are developed. These are based on Stille coupling and, for the first time for TEG-substituted DPP polymers, on direct heteroarylation polymerization. Spectroscopic and electrochemical characterization as well as preliminary tests in photovoltaic cells are reported.

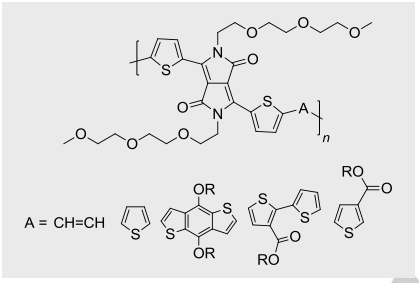

TEG-substituted diketopyrrolopyrrole-based polymers

*Angela Punzi, Francesca Nicoletta, Giuseppe Marzano, Cosimo G. Fortuna, Janardan Dagar, Thomas M. Brown and Gianluca M. Farinola**

Page No. – Page No.

Synthetic routes to TEG-substituted diketopyrrolopyrrole-based low band gap polymers